Laser-induced defects in fused silica by femtosecond IR irradiation

Arnaud Zoubir,[1] Clara Rivero,[2] Rachel Grodsky,[2] Kathleen Richardson,[3] Martin Richardson,[2] Thierry Cardinal,[4] and Michel Couzi[5]

[1]*HORIBA Jobin Yvon SAS, Raman Division, 231 rue de Lille, 59650 Villeneuve d'Ascq, France*

[2]*College of Optics and Photonics/CREOL, UCF, 4000 Central Florida Boulevard, Orlando, Florida 32816, USA*

[3]*School of Material Science and Engineering, Clemson University, 161 Sirrine Hall, Clemson, South Carolina 29634, USA*

[4]*ICMCB-CNRS, Université of Bordeaux 1, 87 Avenue du Docteur Schweitzer 33608 PESSAC cedex, France*

[5]*LPCM-CNRS, Université of Bordeaux 1, 351 Cours de la Liberation, 33405 TALENCE, cedex, France*

(Received 20 September 2005; published 28 June 2006)

Photostructural defects resulting from exposure to intense near-infrared femtosecond radiation is studied in three a-SiO_2 glasses with different impurity levels. The photoinduced defects are studied by UV absorption spectroscopy and are correlated to the structural modifications in the glass matrix through Raman spectroscopy. Information in the dynamics of the defect generation is revealed by the small photon energy of IR femtosecond laser radiation.

DOI: 10.1103/PhysRevB.73.224117 PACS number(s): 78.70.−g, 42.70.−a

I. INTRODUCTION

Radiation-induced defects in fused silica have been studied extensively in a variety of ionizing conditions including β irradiation,[1] energetic ions,[2] protons,[3] γ rays and neutron beam radiation.[4] The generation of such defects by optical radiation has mostly been investigated in the UV range, mostly driven by the microlithography industry, as fused silica has become a material of choice for 248 nm and many 193 nm applications. The study of the dynamics of these defects has also led to an important number of applications, including the fabrication of fiber-Bragg gratings and optical waveguides.

Despite the large number of studies on UV-induced defects in fused silica, few data are available on IR-induced defects generated by ultrashort pulses. Unlike the case of excitation by UV radiation which involves the simultaneous absorption of one to two photons,[5] six photons are required to excite electrons across the ~9 eV band gap of fused silica. Despite a relatively smaller nonlinear absorption cross section in this case, multiphoton ionization is launched due to an extremely high peak power density (tens of TW/cm^2) attainable with an ultrafast laser. Understanding the mechanisms of sub-band gap defect formation in the case of such strongly nonlinear absorption is relevant to several applications, such as the recently demonstrated use of femtosecond (fs) IR lasers to fabricated three-dimensional (3D) optical waveguides,[6] optical memories,[7] and photonic band gap crystals.[8] It is also relevant to high power laser systems constructed for inertial confinement fusion,[4] where fused silica has emerged a key material, due its high optical quality, remarkable thermal shock resistance, and very low absorption.

Although fused silica is a single-component glass, its properties can vary slightly depending on its thermal history and trace levels of impurities. In this study, we considered three commercially available fused silica samples (Suprasil, Infrasil, and EN1027), and studied the variations in their optical properties and response to femtosecond laser radiation. The three samples under investigation have different initial concentrations in those defects, as shown by the preirradiation absorption spectra in Fig. 1: Suprasil and EN1027 have a low concentration in oxygen vacancies, which confers good transparency in the UV, but a high OH-content responsible for the absorption band around 2700 nm. By contrast Infrasil shows no such band in the infrared, but shows high absorption in the UV. Table I shows the variations on the properties and impurity levels of the three samples of interest in this study, prior to irradiation.

II. EXPERIMENTAL SETUP AND SAMPLES

The irradiation was performed using a laser system consisting of a femtosecond Ti:Sapphire oscillator and a regenerative amplifier producing 100 fs pulses at 800 nm at a 1 kHz repetition rate. The writing photon energy (1.55 eV) is much smaller than the band gap of silica (8.9 eV), allowing the laser beam to penetrate deep inside the material and produce volumetric defects. However, due to the multiphoton nature of the absorption leading to the formation of defects, the defect area is highly localized, as the modified material is confined within the focal volume of a highly focused beam. In order to resolve these changes with a standard spectropho-

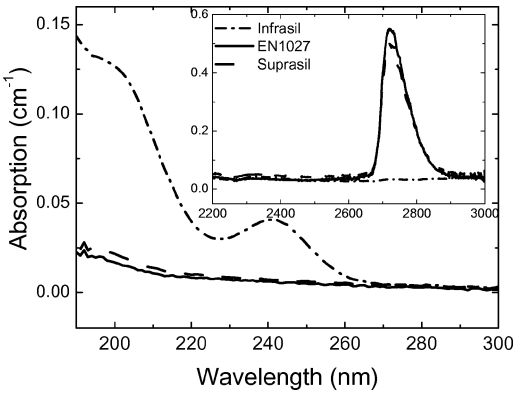

FIG. 1. Absorption spectrum of unexposed Suprasil, EN1027, and Infrasil. The inset represents the IR absorption peaks corresponding to the OH-content of each sample.

TABLE I. Measured optical properties and impurity levels of Infrasil 302, Suprasil 312, and EN1027.

Sample	Density (ρ) (g/cm^3)	n_{633}	n_{514}	Al impurity level (ppm)	OH^- impurity level (ppm)	$\lambda_{cut\text{-}off}$ (nm)
Infrasil 302	2.203	1.45783	1.46518	20	<or=8	210
Suprasil 312	2.201	1.45889	1.46319	0.05	200	165
EN1027[a]	2.201	1.45885	1.46359	unknown	~200	165

[a]EN1027 refers to the code provided to a high purity SiO_2 sample from the CEA Mega Joule Laser project in France.

tometer, a rather large defect volume was produced inside the sample by raster scanning the focal spot (~40 μm in diameter) given by a 10 cm focal length lens, at a scanning speed of 1 mm s^{-1} over a square 1 mm × 1 mm area. The visible-UV change in the absorption coefficient $\Delta\alpha$ was measured only through the irradiated region using a Cary 500 spectrophotometer (Varian). The spontaneous Raman spectra of the different silica samples were also obtained using a micro-Raman configuration. The incoming 514 nm laser excitation was focused inside the bulk of the sample, at the unexposed and exposed defect areas, respectively, via a 100X microscope objective, with a spatial resolution of about 2 μm. The backscattered light was collected and spectrally analyzed with a spectrometer and a CCD detector, with a typical resolution of about 6 cm^{-1}. The Rayleigh line was suppressed with a holographic notch filter. All Raman spectra have been normalized to the intensity of the band near 440 cm^{-1}.

III. RESULTS

In the induced-absorption spectra (Fig. 2), the intrinsic absorption of the samples was subtracted, as to show the change in absorption resulting from laser irradiation. When optical damage was induced, the curves were also corrected for loss associated with Rayleigh scattering, showing as a smooth baseline in $\sim 1/\lambda$,[4] so that the amplitude of the different peaks can be compared.

Two absorption bands were observably induced by the irradiation process in the three samples, as shown in Fig. 2. The peak centered at 214 nm (5.8 eV) and a full width at half maximum (FWHM) of 20 nm (0.54 eV) is attributed to Si E' centers, an unpaired electron in a silicon atom bound to three oxygen atoms ($\equiv Si^{\bullet}$). The peak at 248 nm (5.0 eV) and a FWHM of 16 nm (0.32 eV) corresponds to the $B_2\alpha$ band and is attributed to oxygen-deficient centers [ODC(II)],[9,10] a divalent silicon atom ($=Si^{\bullet\bullet}$).[11] The induced-absorption spectrum also shows the presence of peaks below 190 nm, which is attributed to oxygen deficiency centers: ODC(I), ODC(II) reported in the literature at 7.6 and 6.8 eV, respectively,[11] and nonbridging oxygen hole centers (NBOHC), an oxygen dangling bond ($\equiv Si-O^{\bullet}$) showing a peak also around 6.8 eV. Unfortunately, the UV-range detection limit of the Cary 500 spectrophotometer is 185 nm; however, the nature of these defects was confirmed by the photoluminescence (PL) spectrum. The instrument is from Edinburgh Instruments Ltd. and is equipped with a 450 W xenon lamp, and double monochromator in excitation and detection arms. The PL spectrum obtained with 248 nm excitation (Fig. 3), shows emission bands at 460 nm and below 300 nm corresponding to ODCs, and one at 650 nm corresponding to NBOHCs (although the absorption peak of the latter was not visible on the induced absorption spectrum). Pristine Infrasil samples also show a PL band at 390 nm corresponding to intrinsic ODCs. The density of NBOHCs is surprisingly lower than it

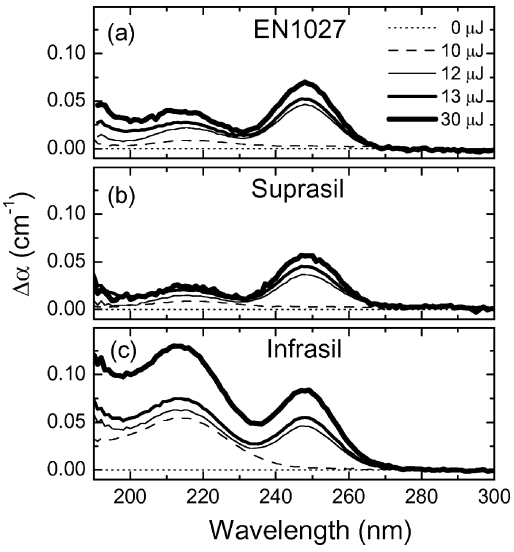

FIG. 2. Absorption change spectrum for varying irradiation pulse energies for (a) EN1027, (b) Suprasil, and (c) Infrasil.

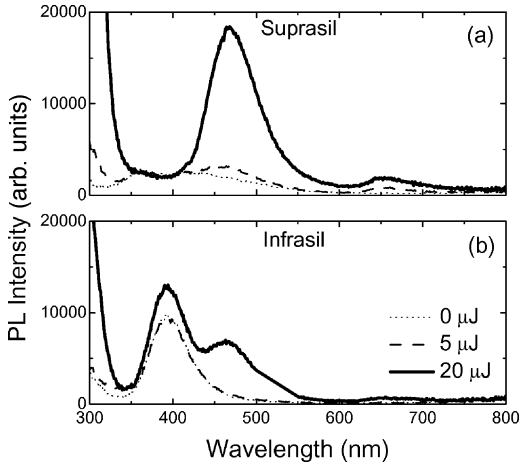

FIG. 3. Photoluminescence spectra of pristine and fs IR laser-irradiated fused silica Suprasil (a) and (b) Infrasil with 248-nm excitation for increasing laser pulse energies.

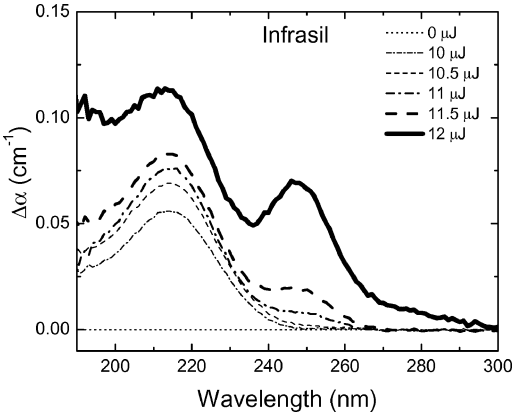

FIG. 4. Absorption change spectrum in Infrasil with smaller pulse energy increment showing the sequential development of Si E' centers (214 nm) and NBOHC (248 nm).

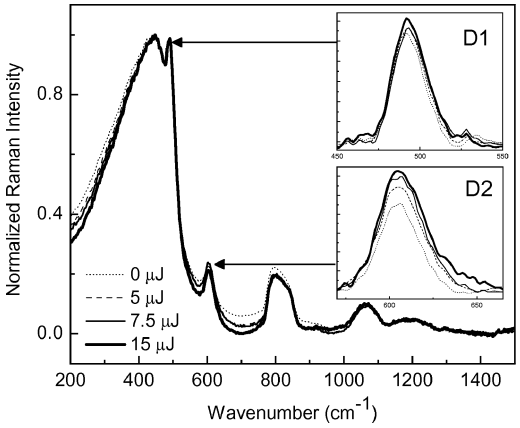

FIG. 5. Raman spectra of pristine and fs IR laser-irradiated fused silica (Infrasil) for increasing laser pulse energies. The insets are magnified images of the D_1 and D_2 lines at 490 cm^{-1} and 606 cm^{-1}, respectively.

was reported in our previous study, where irradiation was performed in similar conditions, and where it was identified as the main induced defect with E' centers.[6] The fused silica samples in this study, however, came from a different source, confirming that another type of fused silica yields yet other defect density ratios than those presented here.

The two photoinduced absorption peaks appear at different laser intensity thresholds. Figure 4 shows the induced absorption in Infrasil irradiated with smaller pulse energy increments than in Fig. 2, as to better resolve the sequential development of the two peaks. Both the Si E' and ODC(II) defects appear to have distinct laser intensity thresholds, I_{th1} and I_{th2}, respectively, at which they are generated. As shown in Fig. 4, for intensities between $I_{th1}=7.96\times10^{12}$ W/cm^2 ($E_p=10$ μJ) and $I_{th2}=9.15\times10^{12}$ W/cm^2 ($E_p=11.5$ μJ), Si E' centers are formed in significant numbers, while the peak amplitude corresponding to ODC(II) remains approximately zero. For intensities of I_{th2} and higher, ODC(II) are induced, and their number increases as the laser intensity is further increased. Although only the shoulder of the peaks below 190 nm is visible on the spectra, they seem to follow the trend of the ODC(II).

Raman spectroscopy has proven an efficient method of characterizing structural modification in fused silica.[12–14] Raman spectra of the irradiated regions are obtained for the three samples (Fig. 5). For clarity, only the spectra of Infrasil are shown since all three samples showed the same trend regarding irradiation, although Infrasil had slightly higher D_1 and D_2 peaks prior to irradiation. The main feature of the spectrum of fused silica is the broad band centered at around 440 cm^{-1}, previously attributed to the Si-O-Si bond rocking and bending in SiO_4 tetrahedra.[15] The two smaller bands at 490 cm^{-1} (D_1) and 606 cm^{-1} (D_2) have been attributed to three- and four-member siloxane rings, respectively, in the silica network.[16] Comparison of these spectra between pristine and irradiated samples reveals two principle trends as the pulse energy is increased: (i) the amplitude of both defect lines D_1 and D_2 increases, and (ii) the width of the main band at 440 cm^{-1} decreases.

IV. DISCUSSION

A large number of mechanisms have been proposed to account for the generation of laser-induced defects. We review here the more commonly reported possible scenarios. A recent review on the subject can be found in Ref. 17. The ODC(I) has been proposed to be precursors of E' centers, according to the reaction (Ref. 18 and 19).

$$\equiv \mathrm{Si}-\mathrm{Si} \equiv \xrightarrow{h\nu} \equiv \mathrm{Si}\cdot + \mathrm{Si} \equiv + e^{-}. \quad (1)$$

Another mechanism, known as the "excitonic" mechanism (generation of a self-trapped exciton, followed by its decay into an E' center and an interstitial oxygen) has also been proposed.[20]

The formation of NBOHCs has been attributed to the rupture of a silanol group (Ref. 21):

$$\equiv \mathrm{Si}-\mathrm{O}-\mathrm{H} \xrightarrow{h\nu} \equiv \mathrm{Si}-\mathrm{O}\cdot + \cdot\mathrm{H}. \quad (2)$$

Another proposed mechanism is the disruption of strained bonds,[5] according to:

$$\equiv \mathrm{Si}-\mathrm{O}-\mathrm{Si} \equiv \xrightarrow{h\nu} \equiv \mathrm{Si}-\mathrm{O}\cdot + \cdot\mathrm{Si} \equiv . \quad (3)$$

It is not clear at this point from what mechanism the ODC(II) originate. However, insight on its precursors can be obtained from the following analysis. Our experimental results indicate that ODC(II) and Si E' are generated at two distinct pulse energy thresholds. At low laser energy (i.e., $I_{th1}<I<I_{th2}$), Si E' centers are predominantly induced and ODC(II) remain negligible through Eq. (1). At high laser energy (i.e., $I>I_{th2}$), the number of generated ODC(II) seems to be roughly the same for all samples, regardless of OH content (Fig. 2), which are the main differences between the three fused silica samples. Laser-induced ODC(II) are therefore thought to arise not from Eq. (2), but from Si-O-Si, as a competing mechanism for Eq. (3).

The photoinduced structural changes occurring in the three fused silica samples were studied using Raman spectroscopy (Fig. 5). The first noticeable change in the spectra as the laser energy is increased is the well-known increase in the amplitude of the D_1 and D_2 defect peaks. This observation has also been reported by Chan *et al.*[14] in the case of IR

femtosecond laser irradiation and is similar to observations made in the case of UV irradiation.[22] It is attributed to the change in ring statistics where sixfold rings transform to threefold and fourfold rings upon laser radiation. The second observation made from the Raman spectra is a decrease of the width of the main 440 cm^{-1} band with increasing irradiation energy. This decrease in bandwidth has also been reported in the case of β irradiation.[1] The frequency of this band relates to the Si-O-Si angle in the glass network, and its width is considered to reflect the width of the Si-O-Si angle distribution. The decrease in the 440 cm^{-1} band can therefore be explained by a decrease in their angular dispersion due to photoinduced ruptures of the strained Si-O-Si bridging bonds which are more likely to break than unstrained bonds. This scenario supports Eq. (3) as the predominant mechanism for generating ODC(II) at $I > I_{th2}$.

NBOHCs have been linked to plastic deformation and cracking of the glass network.[23] In this experiment, the onset of ODC(II) above I_{th2} was seen to correspond to the onset of visible optical damage in the volume of the glass, together with the onset of measurable scattering loss. The damage appears as microscopic cracks formed inside the sample and distributed across the square area scanned by the laser. By contrast, for $I_{th1} < I < I_{th2}$ Si E' centers are generated by laser radiation as shown in the absorption spectra, but no visible damage is observed, and the material remains scatter free. This result may explain our previously reported result that, in fs-IR laser direct writing experiments in fused silica, low-loss waveguides can only be obtained within a narrow pulse energy range.[6] This study showed that, below this operating energy window, the refractive index change was not sufficient to support guiding, whereas above this energy range, high scattering loss prevented practical use of these waveguides.

The key changes produced by fs IR laser irradiation presented in this study have also been reported for various types of treatments of fused silica, such as high-energy particle irradiation,[1–4] high pressure[13] or heat treatment,[12] and UV irradiation.[4,5,24] In all of these cases, color center generation and/or structural modification revealed by Raman spectroscopy have been observed. A major difference outlined in this paper, however, is the selective generation of defects illustrated by Fig. 4, by which Si E' and ODC(II) can be generated separately, depending on the laser intensity. This major difference in the case of intense IR radiation can be understood from the small photon energy of the irradiating laser emission compared to the large electronic transition energies of the defect precursors considered in this paper. The theoretical energies and intensities of optical transitions associated with such point defects in SiO_2 were obtained by Pacchioni *et al.* by *ab initio* calculations on cluster models. They were successfully used to assign some of the absorption bands experimentally observed in α-quartz and amorphous silica.[25]

In the case of UV irradiation, the photon energy is of the same order as the band gap energy calculated for the possible precursors of these defects [intrinsic ODC(I) for E' centers and strained Si-O-Si for ODC(II)]. Kajihara *et al.* showed that, in high-purity synthetic SiO_2 glass irradiated with F_2 laser pulses ($\lambda = 193$ nm), photolysis of the strained Si-O-Si bond takes place via one-photon processes at lower laser power and by consecutive two-step absorption via real intermediate states at higher laser power.[24] In the case of ArF excimer laser irradiation ($\lambda = 248$ nm), two-photon-absorption processes are dominant in the generation of all defects.[5] Whether the one-photon or the two-step process is considered for UV radiation, both defects are bound to appear simultaneously because the two-photon energy is sufficient to excite all precursors at the same time. By contrast, in the IR case, Si E' centers are generated through a five-photon process by Eq. (1) at lower power than ODC(II), which require a six-photon process to excite strained Si-O-Si bonds (Fig. 6). Si E' centers are then expected to be induced at lower power than ODC(II), as revealed by our experiments. This selective disruption of bonds leading to point defects in SiO_2 is reported and explained. It is consistent with the well established multiphoton ionization model,[26] by which energy transfer from excited electrons to the lattice leads to structural changes in the glass matrix. Depending on the laser intensity, different precursors will lead to different defects, resulting in more or less drastic damage morphologies.

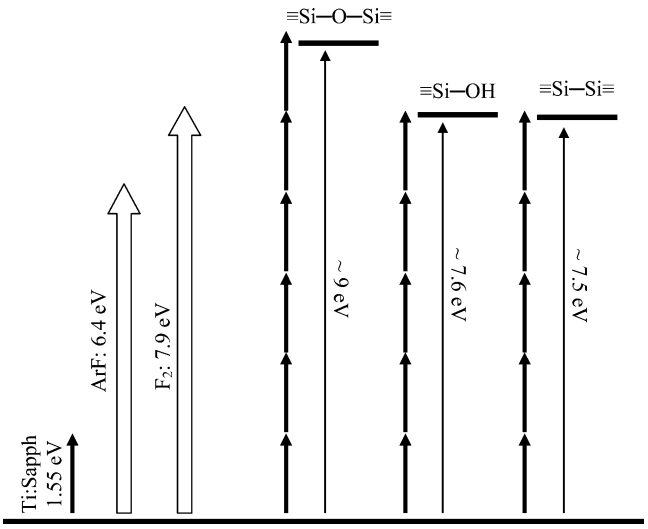

FIG. 6. Schematic representation of the computed electronic transitions of the defect precursors presented in this paper, in comparison with photon energies in the UV and IR case.

V. CONCLUSION

Ultrashort IR laser-induced defects were generated in three fused silica samples having different optical properties. Although the photon energy was far below the material band gap, the induced defects are similar to those reported for UV irradiation. However, in the case of highly multiphoton absorption, the dynamics of defect formation differs in that the two principal defects, Si E' and ODC(II), form at different intensity thresholds. This difference with the UV irradiation case arises from the fact that, with photon energies smaller than the ionization energy of their precursors, both defects can be created separately. Laser-induced generation of ODC(II) was correlated to the onset of visible optical dam-

age in the form of scattering centers in the volume of the sample, whereas the generation of Si E' only left the samples scatter free. Finally, Raman spectroscopy confirmed the generation of threefold and fourfold rings and revealed a decrease in the Si-O-Si angle distribution as a result of the photoinduced disruption of strained bond upon IR femtosecond laser irradiation.

ACKNOWLEDGMENTS

This work was supported by the National Science Foundation Contract No. DMR-9912975 and by the State of Florida. The authors wish to thank G. I. Stegeman for the use of his laser and useful scientific discussions.

[1] B. Boizot, S. Agnello, B. Reynard, R. Boscaino, and G. Petite, J. Non-Cryst. Solids **325**, 22 (2003).
[2] T. Mohanty, N. C. Mishra, S. V. Bhat, P. K. Basu, and D. Kanjilal, J. Phys. D **36**, 3151 (2003).
[3] S. Nagata, S. Yamamoto, K. Toh, B. Tsuchiya, N. Ohtsu, T. Shikama, and H. Naramoto, J. Nucl. Mater., **329-333**, 1507 (2004).
[4] C. D. Marshall, J. A. Speth, and S. A. Payne, J. Non-Cryst. Solids **212**, 59 (1997).
[5] Y. Ikutaa, S. Kikugawa, M. Hirano, and H. Hosono, J. Vac. Sci. Technol. B **18** (6), 28915 (2000).
[6] A. Zoubir, M. Richardson, L. Canioni, A. Brocas, and L. Sarger, J. Opt. Soc. Am. B **22**, 2138 (2005).
[7] E. N. Glezer, M. Milosavljevic, L. Huang, R. J. Finlay, T.-H. Her, J. P. Callan, and E. Mazur, Opt. Lett. **21**, 2023 (1996).
[8] H.-B. Sun, Y. Xu, S. Matsuo, and H. Misawa, Opt. Rev. **6**, 396 (1999).
[9] D. L. Griscom, J. Non-Cryst. Solids **73**, 51 (1985).
[10] R. Tohmon, H. Mizuno, Y. Ohki, K. Sasagane, K. Nagasawa, and Y. Hama, Phys. Rev. B **39**, 1337 (1989).
[11] L. Skuja, J. Non-Cryst. Solids **239**, 16 (1998).
[12] A. E. Geissberger and F. L. Galeener, Phys. Rev. B **28**, 3266 (1983).
[13] R. J. Hemley, H. K. Mao, P. M. Bell, and B. O. Mysen, Phys. Rev. Lett. **57**, 747 (1986).
[14] J. W. Chan, T. R. Huser, S. H. Risbud, and D. M. Krol, Appl. Phys. A **76**, 367 (2003).
[15] F. L. Galeener and A. E. Geissberger, Phys. Rev. B **27**, 6199 (1983).
[16] A. Pasquarello and R. Car, Phys. Rev. Lett. **80**, 5145 (1998).
[17] L. Skuja, M. Hirano, H. Hosono, and K. Kajihara, Phys. Status Solidi A **1**, 15 (2005).
[18] H. Imai, K. Arai, H. Hosono, Y. Abe, T. Arai, and H. Imagawa, Phys. Rev. B **44**, 4812 (1991).
[19] D. L. Griscom, J. Ceram. Soc. Jpn. **99**, 923 (1991).
[20] S. Guizardy, P. Martiny, G. Petitey, P. D'Oliveiraz, and P. Meynadierz, J. Phys.: Condens. Matter **8**, 1281 (1996).
[21] H. Nishikawa, R. Nakamura, Y. Ohki, and Y. Hama, Phys. Rev. B **48**, 15584 (1993).
[22] F. X. Liu, J. Y. Qian, X. L. Wang, L. Liu, and H. Ming, Phys. Rev. B **56**, 3066 (1997).
[23] S. O. Kucheyev and S. G. Demos, Appl. Phys. Lett. **82**, 3230 (2003).
[24] K. Kajihara, Y. Ikuta, and M. Hirano, Appl. Phys. Lett. **81**, 3164 (2002).
[25] G. Pacchioni and G. Ierano, Phys. Rev. B **57**, 818 (1998).
[26] B. C. Stuart, M. D. Feit, A. M. Rubenchik, B. W. Shore, and M. D. Perry, Phys. Rev. Lett. **74**, 2248 (1995).